

Changes of myelin basic protein in the hippocampus of an animal model of type 2 diabetes

Sung Min Nam^{1,2}, Hyun Jung Kwon³, Woosuk Kim¹, Jong Whi Kim¹, Kyu Ri Hahn¹, Hyo Young Jung¹, Dae Won Kim³, Dae Young Yoo^{1,4}, Je Kyung Seong^{1,5}, In Koo Hwang¹, Yeo Sung Yoon^{1,5,*}

¹Department of Anatomy and Cell Biology, College of Veterinary Medicine, and Research Institute for Veterinary Science, Seoul National University, Seoul, Korea

²Department of Anatomy, College of Veterinary Medicine, Konkuk University, Seoul, Korea

³Department of Biochemistry and Molecular Biology, Research Institute of Oral Sciences, College of Dentistry, Gangneung-Wonju National University, Gangneung, Korea

⁴Department of Anatomy, College of Medicine, Soonchunhyang University, Cheonan, Korea

⁵KMPC (Korea Mouse Phenotyping Center), Seoul National University, Seoul, Korea

In this study, we observed chronological changes in the immunoreactivity and expression level of myelin basic protein (MBP), one of the most abundant proteins in the central nervous system, in the hippocampus of Zucker diabetic fatty (ZDF) rats and their control littermates (Zucker lean control; ZLC). In the ZLC group, body weight steadily increased with age; the body weight of the ZDF group, however, peaked at 30 weeks of age, and subsequently decreased. Based on the changes of body weight, animals were divided into the following six groups: early (12-week), middle (30-week), and chronic (52-week) diabetic groups and their controls. MBP immunoreactivity was found in the alveus, strata pyramidale, and lacunosum-moleculare of the CA1 region, strata pyramidale and radiatum of the CA3 region, and subgranular zone, polymorphic layer, and molecular layer of the dentate gyrus. MBP immunoreactivity was lowest in the hippocampus of 12-week-old rats in the ZLC group, and highest in 12-week-old rats in the ZDF group. Diabetes increased MBP levels in the 12-week-old group, while MBP immunoreactivity decreased in the 30-week-old group. In the 52-week-old ZLC and ZDF groups, MBP immunoreactivity was detected in the hippocampus, similar to the 30-week-old ZDF group. Western blot results corroborated with immunohistochemical results. These results suggested that changes in the immunoreactivity and expression of MBP in the hippocampus might be a compensatory response to aging, while the sustained levels of MBP in diabetic animals could be attributed to a loss of compensatory responses in oligodendrocytes.

Keywords: Myelin basic protein, type 2 diabetes, hippocampus, age

Received 13 August 2018; Revised version received 1 October 2018; Accepted 5 October 2018

Type 2 diabetes mellitus (T2DM), one of most prevalent metabolic diseases, is characterized by high levels of insulin and peripheral insulin resistance [1,2]. The hippocampus is a highly insulin-sensitive organ with a high abundance of insulin receptors [1,3]. Accumulating evidence indicates that chronic T2DM leads to cognitive problems, including dementia and Alzheimer's disease [1,4-9]. Among animal models for

T2DM, the Zucker diabetic fatty (ZDF) rats are most frequently used for T2DM models deficient in leptin receptors [10]. Leptin receptor-based animal models shows similar phenotypes with humans including hyperphagia, defective non-shivering thermogenesis, increased efficiency for food utilization, and preferential deposition of energy in adipose tissue [11,12]. ZDF rats start to increase blood glucose levels from 7 weeks of

*Corresponding author: Yeo Sung Yoon, Department of Anatomy and Cell Biology, College of Veterinary Medicine, Seoul National University, Seoul 08826, Korea
Tel: +82-2-880-1264; Fax: +82-2-871-1752; E-mail: ysyoon@snu.ac.kr

age [13,14] and demonstrate a reduction in vascular permeability and expression of tight junction proteins in the hippocampus at 40 weeks of age [15].

T2DM affects the conditions of neurons as well as neuroglia in the hippocampus [16,17]. In the previous study, we observed the microglia in ZDF rats showed activated morphology (*e.g.*, hypertrophied cytoplasm with retracted processes) at 30 weeks of age and we also found the subsequent increases in interleukin-1 β immunoreactive structures in the hippocampus of ZDF rats at 30 weeks of age near the astrocytes and microglia [18]. In addition, we also found the decreases in the integrity of blood-brain barrier and ultrastructural morphology of blood vessels and its adjacent structures at 40 weeks of age [15]. However, there were few reports on the T2DM-induced changes of myelin proteins in the hippocampus.

Myelin basic protein (MBP), which is an essential component of myelin formation, is one of the most abundant proteins in the central nervous system (CNS). Mutations in the MBP gene lead to a lack of compact CNS myelin in mice [19] and rats [20]. MBP is closely associated with cytoskeletal proteins, such as actin, tubulin, tau, and microtubule-associated protein 2 [21-24]. There has been conflicting evidence about changes in MBP expression in the brain of several diseases, including Alzheimer's disease [21-24], scopolamine-induced amnesia [25]. Streptozotocin-induced diabetes also decreased MBP protein levels in the rat cerebral cortex, 1 month after treatment [26] and the level of MBP mRNA in the rat spinal cord after 3 months [27]. However, there are few studies on the effects of T2DM on MBP expression in the hippocampus at various stages of diabetes.

Thus, in the present study, we investigated the changes of MBP immunoreactivity and protein levels in the hippocampus of rats with diabetes at various ages.

Materials and Methods

Experimental animals

Male and female heterozygous (*Lepr*^{f/a+}) Zucker diabetic fatty (ZDF) rats were purchased from Charles River Laboratories (Wilmington, MA) and mated. They were housed under standard conditions with adequate temperature (22°C) and humidity (60%) control, a 12-hr light/12-hr dark cycle, and free access to water and Purina 5008 diet were provided as recommended by

Genetic Models. The handling and care of the animals conformed to the guidelines established to comply with current international laws and policies (NIH Guide for the Care and Use of Laboratory Animals, NIH Publication No. 85-23, 1985, revised 2011) and were approved by the Institutional Animal Care and Use Committee (IACUC) of Seoul National University (Approval number: SNU-120312-10). All experiments were conducted with an effort to minimize the number of animals used and the physiological stress caused by the procedures employed. All experimental procedures were conducted according to ARRIVE guidelines [28].

Check for body weight and blood glucose levels

The genotype of the *f/a* gene was determined by polymerase chain reaction described in our previous study [29]. Based on the genotyping, homozygous ZDF (*Lepr*^{f/a+}) and Zucker lean control (ZLC, *Lepr*^{+/+}) rats were used for diabetic and its control group, respectively. Body weight was measured and blood was sampled by "tail nick" between 9:00 and 11:00 am, using a 27 G needle without fasting. Fed glucose levels before sacrifice were analyzed using a blood glucose monitor (ACCU-CHEK®, Boehringer Mannheim Corp., Indianapolis, IN).

Tissue processing for histology

For immunohistochemical analysis, animals were anesthetized with 2 g/kg urethane (Sigma), before being perfused transcardially with 0.1 M phosphate-buffered saline (PBS; pH 7.4), and then with 4% paraformaldehyde in 0.1 M PBS (pH 7.4). Rat brains were removed, and the brain was postfixed in the same fixative for 12 h. Brains were cryoprotected with an overnight 30% sucrose immersion. Thereafter, 30- μ m-thick brain sections were cut serially in the coronal plane using a cryostat (Leica, Wetzlar, Germany). Sections were collected into six-well plates containing PBS.

Immunohistochemistry for myelin basic protein (MBP)

To obtain accurate data for immunohistochemistry, free-floating sections from all rats were processed carefully under the same conditions as described previously [30]. For each animal, tissue sections were selected with reference to a rat brain atlas [31], between 3.00 and 4.08 mm posterior to the bregma. Ten sections, 90 μ m apart, were sequentially treated with 0.3% hydrogen

peroxide (H_2O_2) in PBS for 30 min and 10% normal horse serum in 0.05 M PBS for 30 min thereafter. The sections were then incubated with a rabbit anti-MBP antibody (1:1,000, Abcam, Cambridge, UK) overnight at 25°C, before being sequentially treated with either biotinylated goat anti-rabbit IgG, or a streptavidin-peroxidase complex (1:200, Vector, Burlingame, CA). Sections were visualized by the reaction with 3,3-diaminobenzidine tetrachloride (Sigma) in 0.1 M Tris-HCl buffer (pH 7.2). The sections were then dehydrated, before being mounted onto gelatin-coated slides, using Canada balsam (Kanto, Tokyo, Japan).

In order to establish the specificity of primary antibody, procedure included the omission of the anti-MBP antibody, goat anti-rabbit, and substitution of normal goat serum for the anti-MBP antibody. As a result, immunoreactivity disappeared completely in tissues. All experiment procedures in the present study were performed under the same circumstance and in parallel.

Data analysis

Analysis of the hippocampal CA1, CA3, and dentate gyrus regions was performed using an image analysis system and ImageJ software v. 1.5 (National Institutes of Health, Bethesda, MD), according to a previously described method [30]. Digital images of the mid-point of hippocampal CA1, CA3, and molecular layer dentate gyrus regions were captured with a BX51 light microscope (Olympus, Tokyo, Japan), equipped with a digital camera (DP72, Olympus) connected to a computer monitor. Images were calibrated into an array of 512×512 pixels corresponding to a tissue area of 1,200 $\mu m \times$ 900 μm (100 \times primary magnification). Each pixel resolution was 256 gray levels, and the intensity of MBP immunoreactivity was evaluated by relative optical density (ROD), which was obtained after transformation of the mean gray level using the following formula: ROD= log(256/mean grayscale level). The ROD of background staining was determined in unlabeled portions of the sections based on the immunohistochemistry staining data with omission of primary antibody using Photoshop CC 2018 software (Adobe Systems Inc., San Jose, CA), and this value was subtracted to correct for nonspecific staining, using ImageJ v. 1.50 software (National Institutes of Health). Data were expressed as a percentage of the 12-week-old

ZLC group values (set to 100%).

Western blot analysis for myelin basic protein (MBP)

To quantify changes in the level of MBP in the hippocampus, ZLC and ZDF rats ($n=4$ per group) were euthanized at 12, 30, and 52 weeks of age. Hippocampal tissue was dissected for western blot analysis as described previously [15]. Briefly, hippocampal tissues were homogenized in 50 mM PBS (pH 7.4), containing 0.1 mM ethylene glycol-bis(2-aminoethyl ether)-N,N,N,N-tetraacetic acid (pH 8.0), 0.2% Nonidet P-40, 10 mM ethylenediaminetetraacetic acid (pH 8.0), 15 mM sodium pyrophosphate, 100 mM β -glycerophosphate, 50 mM NaF, 150 mM NaCl, 2 mM sodium orthovanadate, 1 mM phenylmethylsulfonyl fluoride, and 1 mM dithiothreitol (DTT). After centrifugation, protein levels in the supernatants were determined using a Micro bicinchoninic acid assay kit according to the manufacturer's instructions (Pierce Chemical, Rockford, IL). Aliquots containing 20 μg of total protein were denatured by boiling in loading buffer, which contained 150 mM Tris (pH 6.8), 3 mM DTT, 6% sodium dodecyl sulfate, 0.3% Bromophenol Blue, and 30% glycerol. Each aliquot was loaded onto a polyacrylamide gel. After electrophoresis, proteins were transferred to nitrocellulose membranes (Pall Crop, East Hills, NY), which were then blocked in 5% non-fat dry milk in PBS/0.1% Tween 20 for 45 min, prior to incubation with a rabbit anti-MBP antibody (1:1,000, Abcam). Detection was performed using the peroxidase-conjugated anti-rabbit IgG (Vector) and an enhanced luminol-based chemiluminescent kit (Pierce Chemical). The blots were scanned, and densitometry was performed, using Scion Image software (Scion Corp., Frederick, MD). Blots were stripped and re-probed with an antibody against β -actin for internal loading control. Data were normalized to the β -actin level in each lane.

Statistical analysis

The data shown here represent the mean±standard error of mean (SEM) of experiments performed for each experimental area. Data were analyzed using the GraphPad Prism 5.01 software (GraphPad Software, Inc., La Jolla, CA), and differences among the means were statistically analyzed with two-way ANOVA with Bonferroni's post-hoc test to elucidate differences owing to age and diabetes. Threshold for statistical significance was set to $P<0.05$.

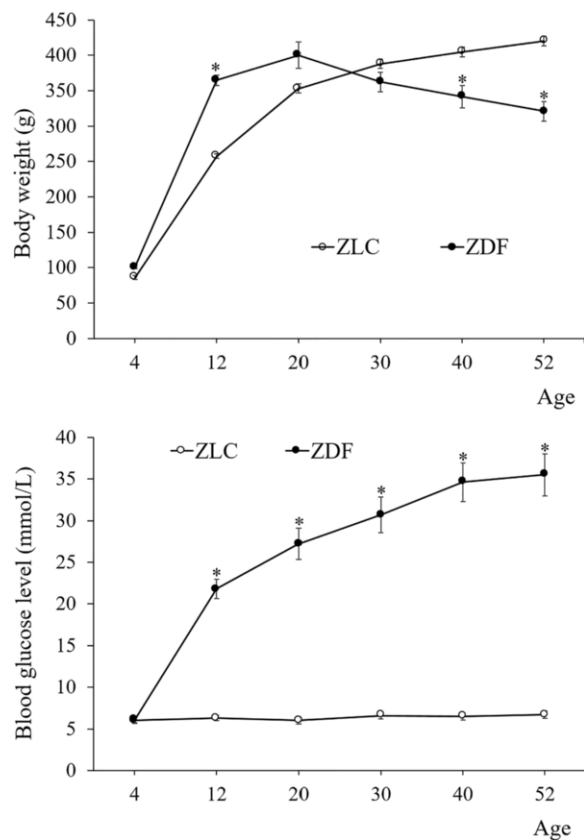


Figure 1. Body weight changes (A) and fed blood glucose levels (B) of Zucker lean control (ZLC) and Zucker diabetic fatty (ZDF) rats, at 4, 12, 20, 30, 40, and 52 months of age ($n=10$). Data shown as mean \pm standard error of mean (SEM). * $P<0.05$ (compared to age-matched ZLC group)

Results

Changes in body weight and blood glucose levels

In the ZLC group, body weight steadily increased with age and weight gain was prominent earlier (*i.e.*, 4 and 20 weeks of age) rather than later (*i.e.*, between 30 and 52 weeks of age). In the ZDF group, body weight, which increased by 20 weeks of age, was significantly higher compared to the age-matched ZLC group. However, body weight gradually decreased in the ZDF group, from 30 to 52 weeks of age. Further, it was significantly lower than that in age-matched rats in the ZLC group (Figure 1). At 40 and 52 weeks of age, the body weight of ZDF rats was lower than 12-week-old rats in the ZDF group.

The blood glucose levels of rats in the ZLC group, which was 6.0–6.7 mmol/L, was similar at all ages. In the ZDF group, blood glucose levels sharply increased between 4 and 12 weeks of age, and steadily increased thereafter until 52 weeks of age (Figure 1).

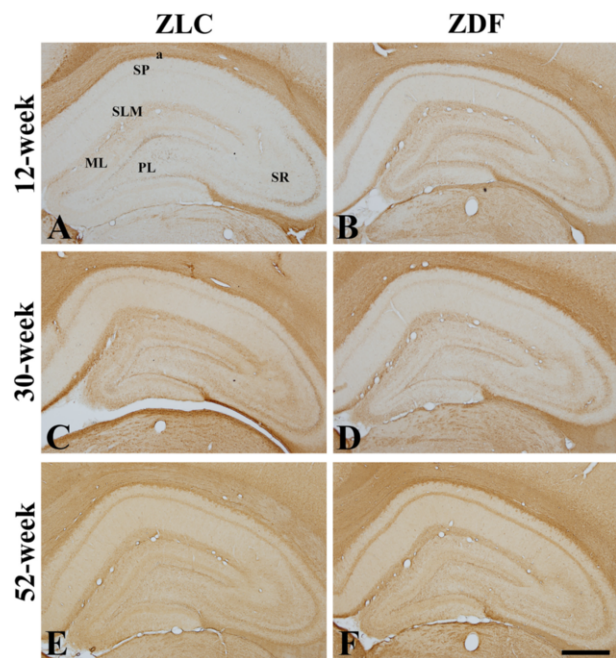


Figure 2. Immunohistochemistry of myelin basic protein (MBP) in the whole hippocampus of Zucker lean control (ZLC; A, C, and E) and Zucker diabetic fatty (ZDF) rats (B, D, and F), at 12 (A and B), 30 (C and D), and 52 (E and F) weeks of age. MBP immunoreactivity is found in the alveus (a), stratum lacunosum moleculare (SML), and stratum pyramidale (SP) of the CA1 region, the stratum radiatum (SR) and SP of the CA3 region, and the subgranular zone, polymorphic layer (PL), and molecular layer (ML) of the dentate gyrus. Note that MBP immunoreactive structures are least abundant in the hippocampus in the 12-week old ZLC rats, and were most abundant in the 12-week-old ZDF or 30-week-old ZLC rats. Scale bar=400 μ m.

Changes in myelin basic protein (MBP) immunoreactivity in the hippocampus

In the 12-week-old ZLC group, MBP immunoreactivity was found in the alveus, strata pyramidale, and lacunosum-moleculare of the CA1 region, the strata pyramidale and radiatum of the CA3 region, and the subgranular zone, polymorphic layer, and molecular layer of the dentate gyrus (Figures 2A, 3A, 3A', 4A, 5A). The MBP immunoreactivity in the hippocampus of the 12-week-old ZDF group was similar to the age-matched ZLC group (Figures 2B, 3D, 3D', 4B, 5B). In the 12-week-old ZDF group, MBP immunoreactivity was particularly higher in the stratum pyramidale of the CA1, stratum radiatum of the CA3, and outer molecular layer of the dentate gyrus (Figures 3G, 4G, 5G).

The MBP immunoreactivity in the hippocampus of rats in the 30-week-old ZLC group was similar to that in the 12-week-old ZDF group (Figures 2C, 3B, 3B', 4C, 5C), except that it was lower in the stratum pyramidale

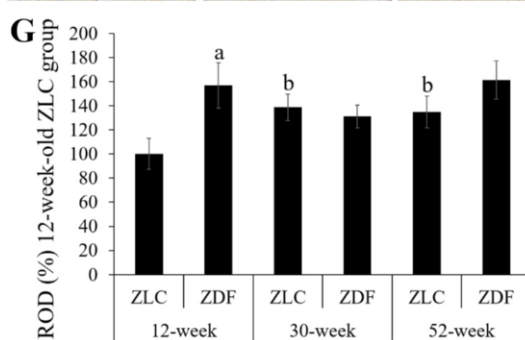
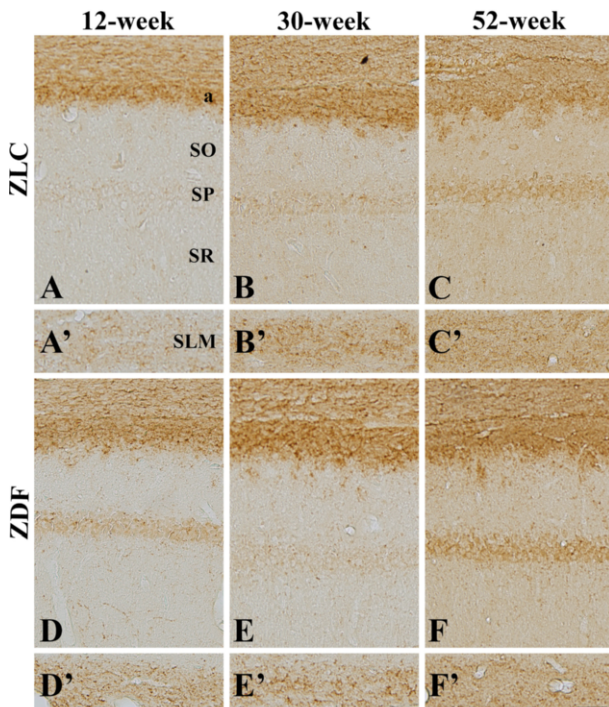


Figure 3. High magnification of myelin basic protein (MBP) immunoreactive structures in the CA1 region (A-F) and stratum lacunosum-moleculare (SLM, A'-F') of Zucker lean control (ZLC; A-C and A'-C') and Zucker diabetic fatty (ZDF; D-F and D'-F') rats, at 12 (A, A', D, and D'), 30 (B, B', E, and E'), and 52 (C, C', F, and F') weeks of age. MBP immunoreactivity is detected in the stratum pyramidale (SP), alveus (a), and SLM of the CA1 region. SO, stratum oriens. Scale bar=50 μ m. G: Relative optical densities (ROD) are expressed as a percentage of the value of the MBP immunoreactivity in the CA1 region in 12-week old ZLC rats ($n=5$ in each group). Data are analyzed with a two-way analysis of variance, followed by a Bonferroni's post-hoc test (^a $P<0.05$, significantly different from the ZLC group, ^b $P<0.05$, significantly different from the 12-week-old group). Data shown as mean \pm standard error of mean (SEM).

of the CA1 region in the 30-week-old ZLC group (Figure 3G). Further, the MBP immunoreactivity in the 30-week-old ZDF group was also lower in the stratum pyramidale of the CA3 region and molecular layer of the dentate gyrus, compared to that in the 12-week-old ZDF group and age-matched ZLC group (Figures 2D, 3E, 3E', 3G, 4D, 4G, 5D, 5G).

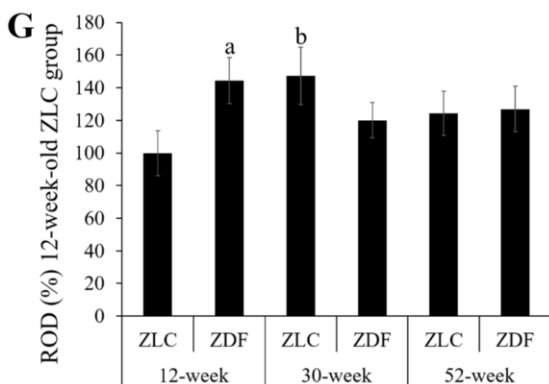
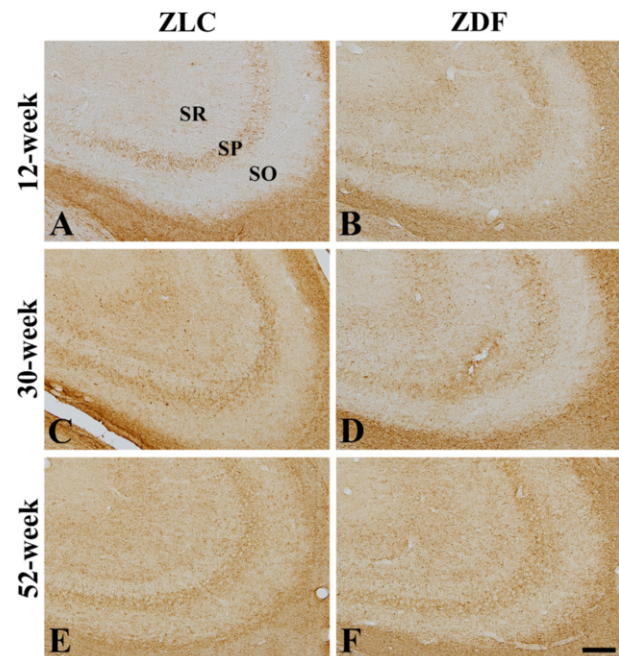


Figure 4. High magnification of myelin basic protein (MBP) immunoreactive structures in the CA3 region of Zucker lean control (ZLC; A, C, and E) and Zucker diabetic fatty (ZDF; B, D, and F) rats at 12 (A and B), 30 (C and D), and 52 (E and F) weeks of age. MBP immunoreactivity is detected in the stratum pyramidale (SP) and radiatum (SR) of the CA3 region. SO, stratum oriens. Scale bar=50 μ m. G: Relative optical densities (ROD) are expressed as a percentage of the value of the MBP immunoreactivity in the CA3 region in the 12-week-old ZLC group ($n=5$ in each group). Data are analyzed by a two-way analysis of variance followed by a Bonferroni's post-hoc test (^a $P<0.05$, significantly different from the ZLC group, ^b $P<0.05$, significantly different from the 12-week-old group). Data shown as mean \pm standard error of mean (SEM).

At 52 weeks of age, the MBP immunoreactivity in the hippocampus of rats in the ZLC group, was similar to the 30-week-old ZLC group, except that it had decreased in the stratum lacunosum-moleculare of CA1 region (Figures 2E, 3C, 3C', 3G, 4E, 4G, 5E, 5G). Further, although the MBP immunoreactivity in the 52-week-old ZDF group was similar to the age-matched ZLC group,

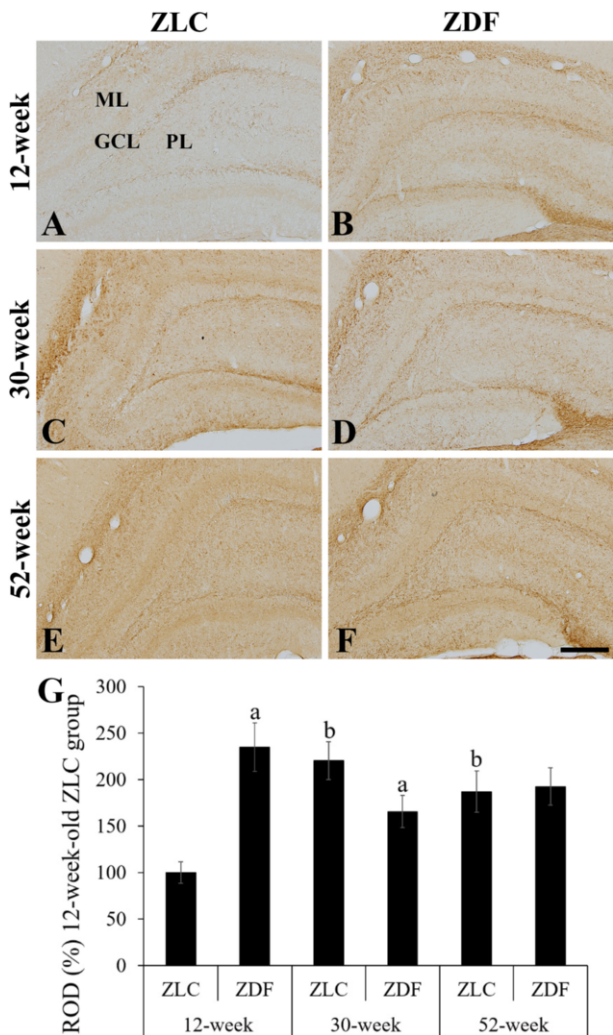


Figure 5. High magnification of myelin basic protein (MBP) immunoreactive structures in the dentate gyrus of Zucker lean control (ZLC; A, C, and E) and Zucker diabetic fatty (ZDF; B, D, and F) rats at 12 (A and B), 30 (C and D), and 52 (E and F) weeks of age. MBP immunoreactivity is observed in the subgranular zone, polymorphic layer (PL), and molecular layer (ML) of the dentate gyrus. GCL, granule cell layer. Scale bar=100 μ m. G: Relative optical densities (ROD) are expressed as a percentage of the value of the MBP immunoreactivity in the dentate gyrus in the 12-week-old ZLC group ($n=5$ in each group). Data are analyzed using a two-way analysis of variance followed by a Bonferroni's post-hoc test ($^aP<0.05$, significantly different from the ZLC group, $^bP<0.05$, significantly different from the 12-week-old group). Data shown as mean \pm standard error of mean (SEM).

it was higher in the stratum pyramidale of the CA1 region compared to the age-matched ZLC group (Figures 2F, 3F, 3F', 3G, 4F, 4G, 5F, 5G).

Changes in the level of myelin basic protein (MBP) in the hippocampus

The level of MBP was higher in the hippocampus of

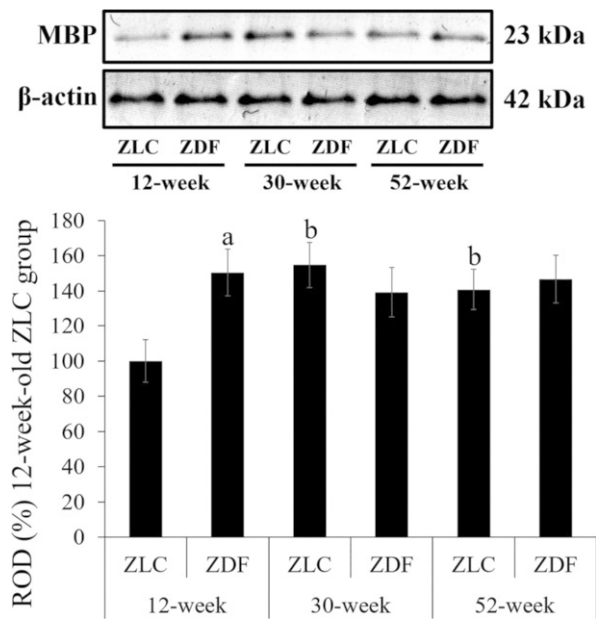


Figure 6. Western blot analysis. Protein levels are expressed as a percentage of the level of myelin basic protein (MBP), normalized to the β -actin protein level, in the hippocampal homogenates of Zucker lean control (ZLC) and Zucker diabetic fatty (ZDF) rats, at 12, 30, and 52 weeks of age. G: Relative optical densities (ROD) are expressed as a percentage of the value of the MBP protein band in the dentate gyrus in the 12-week-old ZLC group ($n=5$ in each group). Data are analyzed using a two-way analysis of variance followed by a Bonferroni's post-hoc test ($^aP<0.05$, significantly different from the ZLC group, $^bP<0.05$, significantly different from the 12-week-old group). Data shown as mean \pm standard error of mean (SEM).

the 12-week-old ZDF group, compared to the 12-week-old ZLC group. Except this, the level of MBP in the hippocampus did not significantly differ between groups, although it was slightly, but not significantly, increased in the 52-week-old ZDF group compared to the age-matched ZLC group (Figure 6).

Discussion

In the present study, we investigated changes in the body weight and blood glucose levels of ZLC and ZDF rats, at various ages. Compared to ZLC rats, the blood glucose levels dramatically increased in ZDF rats at 4–12 weeks of age, thereafter, steadily increasing and tapering at 52 weeks of age. However, in ZDF rats, body weight peaked at 20 weeks of age and gradually decreased thereafter, although blood glucose levels steadily increased by 52 weeks of age. This result corroborated with previous studies, which demonstrated that the difference in body weight and body mass index

between ZDF and ZCL rats had disappeared at 15 weeks of age [32,33]. Another study, however, reported that a higher body weight in ZLC rats, compared to ZDF rats, at 24 weeks of age [34]. Based on this observation, we divided the animals with the following three subgroups: early diabetic (12 weeks of age), chronic diabetic (30 weeks of age), and late diabetic (52 weeks of age) groups, and assessed MBP expression in the hippocampus.

The distribution pattern of MBP was consistent with previous studies, where MBP immunoreactivity was found in the alveus, stratum pyramidale, and stratum lacunosum-moleculare of the CA1 region, the stratum pyramidale and radiatum of the CA3 region, and the molecular layer, subgranular zone, and polymorphic layer of the dentate gyrus [25,35,36]. In the ZLC rats, MBP immunoreactivity peaked at 30 weeks of age, before decreasing at 52 weeks. This result was in line with a previous study reporting a significant reduction in MBP immunoreactivity in the hippocampal CA1 region of senescence-accelerated mice, at 5 or 10 months of age, in comparison to age-matched control mice [35]. In addition, the stratum lacunosum-moleculare is the most susceptible regions to scopolamine-induced decreases in MBP expression [25]. Fewer and shorter myelinated fibers are visible in stratum lacunosum-moleculare of CA1 region in control and Down syndrome patients with age [37]. In the present study, MBP immunoreactivity transiently decreased in ZDF rats in the stratum lacunosum-moleculare and molecular layer of dentate gyrus at 30 weeks of age, compared to the age-matched ZLC group. In addition, our proteomic approach demonstrated the reduction of MBP expression in the hippocampal homogenates at 40 weeks of age [38]. However, we failed to observe any significant changes in MBP immunoreactivity in the hippocampus at 52 weeks, although MBP immunoreactivity was higher in the stratum pyramidale of CA1 region in ZDF rats. Chronic T2DM reduced cognitive function, with or without Alzheimer's disease pathology [39,40]. In addition, Hussain et al. quantitatively observed the substantial neuronal loss in the cerebral cortex of a young rat model of T2DM in comparison to age-matched healthy Wistar rats [41]. In the previous studies, we also demonstrated the reduction of integrity of blood-brain barrier [15] and disarrangement of myelin in the hippocampal tissue [38]. Further, several studies have reported that the MBP level and its mRNA expression increased in the brain in Alzheimer's disease [42-44].

However, MBP immunoreactivity did not significantly change with age in ZDF rats. This suggested that diabetes may decrease the plasticity of oligodendrocytes in the hippocampus and may be associated with reduction in regenerating process in various insults with T2DM. In the peripheral region, ischemia upregulated the expression of MBP in the hindlimbs limbs of wild-type mice, but no significant changes were observed in T2DM mice [45]. Similarly, in the central region, compared to non-DM ischemic rats, MBP immunoreactive density sharply decreased in the hippocampus and subcortical white matter of rats, at 13 months of age, due to diabetes and ischemia, which were induced by nicotinamide and streptozotocin [46]. In the T1DM rats induced by streptozotocin, MBP protein levels were similarly observed in the cerebral cortex of rats in the control and diabetic rats at 20 weeks after STZ treatment [47]. In the peripheral system, MBP expression showed conflict results in streptozotocin-induced T1DM. MBP expression levels are decreased in the sciatic nerve of diabetic rats [47,48], while similar MBP expression levels were found in the sciatic nerve 4 weeks after streptozotocin treatment [48]. In isolated primary Schwann cells, hyperglycemia significantly decreased the expression of MBP and this effect has been blocked by insulin treatment [48]. Diabetes or hyperglycemia decelerates the regenerative neurogenesis in the stroke [46] and stab wound injury [49].

In conclusion, MBP immunoreactivity changed in the hippocampus of non-diabetic control aged animals, but not in the diabetic animals. The sustained expression of MBP in the diabetic rats may be associated with the decrease in the plasticity of oligodendrocytes in the hippocampus.

Acknowledgments

This work was supported by Basic Science Research Program through the National Research Foundation of Korea (NRF) funded by the Ministry of Education (NRF-2015R1D1A1A01059314) and was supported by Korea Mouse Phenotyping Project (NRF-2015M3A9D5A01076747) of the Ministry of Science, ICT and Future Planning through the National Research Foundation (NRF), Korea. This study was partially supported by the Research Institute for Veterinary Science, Seoul National University.

Conflict of interests The authors declare that there is no financial conflict of interests to publish these results.

References

- Benedict C, Grillo CA. Insulin Resistance as a Therapeutic Target in the Treatment of Alzheimer's Disease: A State-of-the-Art Review. *Front Neurosci* 2018; 12: 215.
- Salunkhe VA, Veluthakal R, Kahn SE, Thurmond DC. Novel approaches to restore beta cell function in prediabetes and type 2 diabetes. *Diabetologia* 2018; 61(9): 1895-1901.
- Derakhshan F, Toth C. Insulin and the brain. *Curr Diabetes Rev* 2013; 9(2): 102-116.
- Kalaria RN. Neurodegenerative disease: Diabetes, microvascular pathology and Alzheimer disease. *Nat Rev Neurol* 2009; 5(6): 305-306.
- Bauduceau B, Doucet J, Bordier L, Garcia C, Dupuy O, Mayaudon H. Hypoglycaemia and dementia in diabetic patients. *Diabetes Metab* 2010; 36 Suppl 3: S106-S111.
- Ravona-Springer R, Schnaider-Beeri M. The association of diabetes and dementia and possible implications for nondiabetic populations. *Expert Rev Neurother* 2011; 11(11): 1609-1617.
- De La Monte SM. Metabolic derangements mediate cognitive impairment and Alzheimer's disease: role of peripheral insulin-resistance diseases. *Panminerva Med* 2012; 54(3): 171-178.
- McCrimmon RJ, Ryan CM, Frier BM. Diabetes and cognitive dysfunction. *Lancet* 2012; 379(9833): 2291-2299.
- Yates KF, Sweat V, Yau PL, Turchiano MM, Convit A. Impact of metabolic syndrome on cognition and brain: a selected review of the literature. *Arterioscler Thromb Vasc Biol* 2012; 32(9): 2060-2067.
- Wang B, Chandrasekera PC, Pippin JJ. Leptin- and leptin receptor-deficient rodent models: relevance for human type 2 diabetes. *Curr Diabetes Rev* 2014; 10(2): 131-145.
- Bray GA. The Zucker-fatty rat: a review. *Fed Proc* 1977; 36(2): 148-153.
- Chua SC Jr, Chung WK, Wu-Peng XS, Zhang Y, Liu SM, Tartaglia L, Leibel RL. Phenotypes of mouse diabetes and rat fatty due to mutations in the OB (leptin) receptor. *Science* 1996; 271(5251): 994-996.
- Peterson R, Shaw W, Neel M, Little L, Eichberg J. Zucker diabetic fatty rat as a model for non-insulin-dependent diabetes mellitus. *ILAR J* 1990; 32(3): 16-19.
- Schmidt RE, Dorsey DA, Beaudet LN, Peterson RG. Analysis of the Zucker Diabetic Fatty (ZDF) type 2 diabetic rat model suggests a neurotrophic role for insulin/IGF-I in diabetic autonomic neuropathy. *Am J Pathol* 2003; 163(1): 21-28.
- Yoo DY, Yim HS, Jung HY, Nam SM, Kim JW, Choi JH, Seong JK, Yoon YS, Kim DW, Hwang IK. Chronic type 2 diabetes reduces the integrity of the blood-brain barrier by reducing tight junction proteins in the hippocampus. *J Vet Med Sci* 2016; 78(6): 957-962.
- Dhananjayan K, Gunawardena D, Hearn N, Sonntag T, Moran C, Gyengesi E, Srikanth V, Münnich G. Activation of Macrophages and Microglia by Interferon- α and Lipopolysaccharide Increases Methylglyoxal Production: A New Mechanism in the Development of Vascular Complications and Cognitive Decline in Type 2 Diabetes Mellitus? *J Alzheimers Dis* 2017; 59(2): 467-479.
- Maldonado-Ruiz R, Montalvo-Martínez L, Fuentes-Mera L, Camacho A. Microglia activation due to obesity programs metabolic failure leading to type two diabetes. *Nutr Diabetes* 2017; 7(3): e254.
- Hwang IK, Choi JH, Nam SM, Park OK, Yoo DY, Kim W, Yi SS, Won MH, Seong JK, Yoon YS. Activation of microglia and induction of pro-inflammatory cytokines in the hippocampus of type 2 diabetic rats. *Neurol Res* 2014; 36(9): 824-832.
- Readhead C, Takasaki N, Shine HD, Saavedra R, Sidman R, Hood L. Role of myelin basic protein in the formation of central nervous system myelin. *Ann N Y Acad Sci* 1990; 605: 280-285.
- Carré JL, Goetz BD, O'Connor LT, Bremer Q, Duncan ID. Mutations in the rat myelin basic protein gene are associated with specific alterations in other myelin gene expression. *Neurosci Lett* 2002; 330(1): 17-20.
- Boggs JM, Rangaraj G. Interaction of lipid-bound myelin basic protein with actin filaments and calmodulin. *Biochemistry* 2000; 39(26): 7799-7806.
- Hill CM, Libich DS, Harauz G. Assembly of tubulin by classic myelin basic protein isoforms and regulation by post-translational modification. *Biochemistry* 2005; 44(50): 16672-16683.
- Tompa P. The interplay between structure and function in intrinsically unstructured proteins. *FEBS Lett* 2005; 579(15): 3346-3354.
- Bamm VV, Ahmed MA, Harauz G. Interaction of myelin basic protein with actin in the presence of dodecylphosphocholine micelles. *Biochemistry* 2010; 49(32): 6903-6915.
- Park JH, Choi HY, Cho JH, Kim IH, Lee TK, Lee JC, Won MH, Chen BH, Shin BN, Ahn JH, Tae HJ, Choi JH, Chung JY, Lee CH, Cho JH, Kang IJ, Kim JD. Effects of Chronic Scopolamine Treatment on Cognitive Impairments and Myelin Basic Protein Expression in the Mouse Hippocampus. *J Mol Neurosci* 2016; 59(4): 579-589.
- Cermenati G, Giatti S, Audano M, Pesaresi M, Spezzano R, Caruso D, Mitro N, Melcangi RC. Diabetes alters myelin lipid profile in rat cerebral cortex: Protective effects of dihydroprogesterone. *J Steroid Biochem Mol Biol* 2017; 168: 60-70.
- Pesaresi M, Giatti S, Calabrese D, Maschi O, Caruso D, Melcangi RC. Dihydroprogesterone increases the gene expression of myelin basic protein in spinal cord of diabetic rats. *J Mol Neurosci* 2010; 42(2): 135-139.
- Kilkenny C, Browne WJ, Cuthill IC, Emerson M, Altman DG. Improving bioscience research reporting: the ARRIVE guidelines for reporting animal research. *PLoS Biol* 2010; 8(6): e1000412.
- Hwang IK, Yi SS, Kim YN, Kim IY, Lee IS, Yoon YS, Seong JK. Reduced hippocampal cell differentiation in the subgranular zone of the dentate gyrus in a rat model of type II diabetes. *Neurochem Res* 2008; 33(3): 394-400.
- Nam SM, Kim JW, Yoo DY, Jung HY, Chung JY, Kim DW, Hwang IK, Yoon YS. Hypothyroidism increases cyclooxygenase-2 levels and pro-inflammatory response and decreases cell proliferation and neuroblast differentiation in the hippocampus. *Mol Med Rep* 2018; 17(4): 5782-5788.
- Paxinos G, Watson C. The rat brain in stereotaxic coordinates. Elsevier Academic Press, Amsterdam, 2007.
- Muñoz MC, Barberà A, Domínguez J, Fernández-Alvarez J, Gomis R, Guinovart JJ. Effects of tungstate, a new potential oral antidiabetic agent, in Zucker diabetic fatty rats. *Diabetes* 2001; 50(1): 131-138.
- Torres TP, Catlin RL, Chan R, Fujimoto Y, Sasaki N, Printz RL, Newgard CB, Shiota M. Restoration of hepatic glucokinase expression corrects hepatic glucose flux and normalizes plasma glucose in zucker diabetic fatty rats. *Diabetes* 2009; 58(1): 78-86.
- Povlsen JA, Løfgren B, Dalgaard C, Birkler RI, Johannsen M, Støstrup NB, Bøtker HE. Protection against myocardial ischemia-reperfusion injury at onset of type 2 diabetes in Zucker diabetic fatty rats is associated with altered glucose oxidation. *PLoS One* 2013; 8(5): e64093.
- Tanaka J, Okuma Y, Tomobe K, Nomura Y. The age-related degeneration of oligodendrocytes in the hippocampus of the senescence-accelerated mouse (SAM) P8: a quantitative immunohistochemical study. *Biol Pharm Bull* 2005; 28(4): 615-618.
- Ahn JH, Chen BH, Shin BN, Cho JH, Kim IH, Park JH, Lee JC, Tae HJ, Lee YL, Lee J, Byun K, Jeong GB, Lee B, Kim SU, Kim YM, Won MH, Choi SY. Intravenously Infused F3.Olig2 Improves Memory Deficits via Restoring Myelination in the Aged

- Hippocampus Following Experimental Ischemic Stroke. *Cell Transplant* 2016; 25(12): 2129-2144.
37. Ábrahám H, Vincze A, Veszprémi B, Kravák A, Gömöri É, Kovács GG, Seress L. Impaired myelination of the human hippocampal formation in Down syndrome. *Int J Dev Neurosci* 2012; 30(2): 147-158.
 38. Nam SM, Yoo DY, Kwon HJ, Kim JW, Jung HY, Kim DW, Han HJ, Won MH, Seong JK, Hwang IK, Yoon YS. Proteomic approach to detect changes in hippocampal protein levels in an animal model of type 2 diabetes. *Neurochem Int* 2017; 108: 246-253.
 39. Winocur G, Greenwood CE. Studies of the effects of high fat diets on cognitive function in a rat model. *Neurobiol Aging* 2005; 26 Suppl 1: 46-49.
 40. Moroz N, Tong M, Longato L, Xu H, de la Monte SM. Limited Alzheimer-type neurodegeneration in experimental obesity and type 2 diabetes mellitus. *J Alzheimers Dis* 2008; 15(1): 29-44.
 41. Hussain S, Mansouri S, Sjöholm Å, Patrone C, Darsalia V. Evidence for cortical neuronal loss in male type 2 diabetic Goto-Kakizaki rats. *J Alzheimers Dis* 2014; 41(2): 551-560.
 42. Macq AF, Goossens F, Maloteaux JM, Octave JN. Overexpression of the myelin basic protein RNA in the cortex of a patient with Alzheimer's disease. *Acta Neurol Belg* 1989; 89(3-4): 316.
 43. Roher AE, Weiss N, Kokjohn TA, Kuo YM, Kalback W, Anthony J, Watson D, Luehrs DC, Sue L, Walker D, Emmerling M, Goux W, Beach T. Increased A beta peptides and reduced cholesterol and myelin proteins characterize white matter degeneration in Alzheimer's disease. *Biochemistry* 2002; 41(37): 11080-11090.
 44. Gil V, Nicolas O, Mingorance A, Urefía JM, Tang BL, Hirata T, Sáez-Valero J, Ferrer I, Soriano E, del Río JA. Nogo-A expression in the human hippocampus in normal aging and in Alzheimer disease. *J Neuropathol Exp Neurol* 2006; 65(5): 433-444.
 45. Schiekofer S, Galasso G, Sato K, Kraus BJ, Walsh K. Impaired revascularization in a mouse model of type 2 diabetes is associated with dysregulation of a complex angiogenic-regulatory network. *Arterioscler Thromb Vasc Biol* 2005; 25(8): 1603-1609.
 46. Zhang L, Chopp M, Zhang Y, Xiong Y, Li C, Sadry N, Rhaleb I, Lu M, Zhang ZG. Diabetes Mellitus Impairs Cognitive Function in Middle-Aged Rats and Neurological Recovery in Middle-Aged Rats After Stroke. *Stroke* 2016; 47(8): 2112-2118.
 47. Kawashima R, Kojima H, Nakamura K, Arahat A, Fujita Y, Tokuyama Y, Saito T, Furudate S, Kurihara T, Yagishita S, Kitamura K, Tamai Y. Alterations in mRNA expression of myelin proteins in the sciatic nerves and brains of streptozotocin-induced diabetic rats. *Neurochem Res* 2007; 32(6): 1002-1010.
 48. Rachana KS, Manu MS, Advirao GM. Insulin influenced expression of myelin proteins in diabetic peripheral neuropathy. *Neurosci Lett* 2016; 629: 110-115.
 49. Dorsemans AC, Soulé S, Weger M, Bourdon E, Lefebvre d'Hellencourt C, Meilhac O, Diotel N. Impaired constitutive and regenerative neurogenesis in adult hyperglycemic zebrafish. *J Comp Neurol* 2017; 525(3): 442-458.